An innovating gamma-spectroscopy experimental technique for measuring the integral capture cross section of actinides

Pierre Leconte, Jean-Pascal Hudelot*, Muriel Antony, David Bernard
Commissariat à l'énergie atomique, Nuclear Energy Division,
13115 Saint-Paul-Lez-Durance Cedex, FRANCE

Abstract

This paper describes innovative measurements of integral radiative capture rates of minor actinides, performed in the MINERVE facility. They aim at resolving potential discrepancies on capture cross sections, especially in the framework of nuclear safety and of waste management.

For this purpose, specific samples containing pure isotopes mixed in natural UO_2 pellets have been fabricated. The measurements consist of γ-ray spectrometry on irradiated fuel samples in order to determine the reaction rates with their specific activities and the corresponding spectral indices, defined as the ratio of (n,γ) capture rate to the total fission rate.

This study focuses on the following isotopes : ^{232}Th, ^{237}Np, ^{242}Pu and presents the comparison of experimental results with calculation results obtained with deterministic (APOLLO2) and probabilistic (MCNP4C2) codes, with the JEF2.2, ENDF/B-VI.8 and JEFF3.1 data libraries.

KEYWORDS: γ-ray spectrometry, actinide, OSMOSE program, MINERVE facility, spectral indices, oscillation samples

1. Introduction

Within the frameworks of plutonium recycling, transmutation studies, waste management, increase of the fuel loading length and nuclear safety, the control and the improvement of the accuracy of nuclear data becomes necessary for relevant isotopes.

For this purpose, the OSMOSE program [1] made with EDF and the US Department of Energy, has been undertaken in order to determine integral absorption rates of minor actinides, by the oscillation technique in the MINERVE facility of CEA Cadarache. It aims at understanding and resolving potential discrepancies between calculated and measured values. In this frame, specific samples have been fabricated, containing pure isotopes mixed in natural UO_2 sintered pellets and sheathed within two waterproof Zy4 clad. Due to the rarity of some materials and the lack of experimental data related to, these results are of major interest for the qualification of cross sections data, particularly for the new European library JEFF3.1.

In parallel, a technique for measuring the spectral indices $C_X(n,\gamma) / F_{tot}$, defined as the ratio of the (n,γ) capture rate on "X" to the total fission rate, has been developed and improved, based on past studies related to the modified conversion ratio (capture rate on ^{238}U over the total fission rate) [2]. The measurement consists of γ-ray spectrometry applied directly on irradiated fuel samples, in order to determine the capture and fission rates with their specific activities. The feasibility of the experiment depends on some properties of the reaction

* Corresponding author, Tel. +334 42 25 43 58, Fax. +334 42 25 78 76, E-mail: jean-pascal.hudelot@cea.fr

products, as the radioactive periods, the γ-ray emission probabilities and the fission yields.

This study focuses on the best adapted actinides for this technique: ^{232}Th, ^{237}Np and ^{242}Pu. First, the principal of the experiment is given, and the core configuration, the experimental γ-ray spectrometry device, the theoretical approach of the problem, are described. Then, the different steps of the measurement - net peak area measurements, decay and dead time corrections, efficiency calibration of the Germanium detector, calculation of efficiency transfers and average fission yields - are detailed. In parallel, the propagation of all the sources of uncertainty is presented. Finally, the spectral indices are given and compared with reference continuous energy probabilistic MCNP code [3] calculations and with 172 energy group deterministic APOLLO2 code [4] calculations, using the JEF2.2, ENDF/B-VI.8 and JEFF3.1 data libraries.

2. Principle of the experiment

2.1 Core configuration

In the frame of the OSMOSE program [1] [5] [6], the 'R1-UO2' core configuration, representative of a UO_2-PWR spectrum was loaded. It consists of 776 UO_2 (enriched at 3% in ^{235}U) fuel pins in a lattice with a square pitch of 1.26 cm (Fig. 1).

Figure 1 : Radial view of the R1-UO2 core configuration of MINERVE

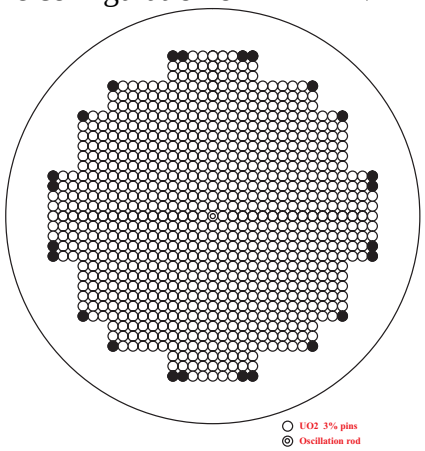

Figure 2 : Top view of the experimental γ-ray spectrometry device

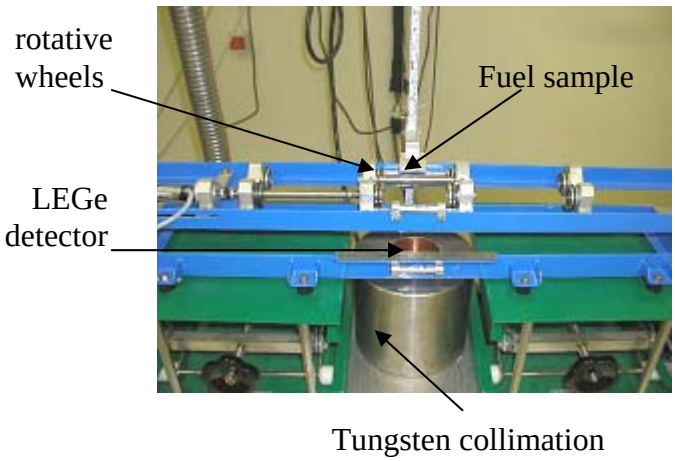

Each sample is introduced in a stainless steel cylindrical tube with a 12 mm diameter, and is axially centered with respect to the fuel lattice between aluminum cylinders.

2.2 Experimental γ-ray spectrometry device

The experimental device is made of a LEGe detector with a high resolution at low energies (0.536 keV at 121.7 keV) and of a Digital Signal Processor 2060 [7], allowing high activity measurements (up to 10^5 counts per second with an error below 1%). A 50 mm thick tungsten collimation is set around the detector to prevent from background activity with 1 mm thick copper-cadmium layers to prevent from fluorescence X-rays. At last, a specific holder for the position and rotation of samples has been used (see Fig. 2).

2.3 Equations of the problem

The principle of the experiment is to measure radioactive reaction products which have been formed during the irradiation, detecting characteristic γ-rays following their decay.

Resolving the evolution equations during the irradiation, cooling and counting phases of the experiment, the spectral indices, i.e. the capture rate on X per unit of fission, are [2] :

$$\frac{C_x}{F} = Y \frac{A(E_c)}{A(E_f)} \frac{I_\gamma(E_f)}{I_\gamma(E_c)} \frac{R^p(E_f)}{R^p(E_c)} \frac{T(E_f)}{T(E_c)} \qquad (1)$$

with : $I_\gamma(E)$ = γ-ray emission probability of the reaction product with the energy E,
$R^p(E)$ = detection efficiency for a point source with the energy E,
$T(E)$ = efficiency transfer correction,
Y = average fission yield over all fissionable isotopes,
$A(E) = N(E)/t_r \times C_\theta C_{dec}$ = saturated count rate of the γ-ray with the energy E, where : $N(E)$ is the net area of the photopeak with the energy E, t_r is the real time of measurement, and C_θ and C_{dec} are respectively the dead time correction factor and the decay correction factor.

The saturated count rates and detection efficiencies are measured. Some nuclear data - fission yields, radioactive periods and γ-ray emission probabilities - are also required. Furthermore, reaction rate calculations have to be performed to estimate the average fission yields and the efficiency transfer corrections. All will be described in the next sections.

The overall uncertainty on the spectral indices is simply obtained from the variance propagation relation, given at the first order by the following equation (3):

$$u^2\left(\frac{C_x}{F}\right)\Big/\left(\frac{C_x}{F}\right)^2 = u^2(Y)/Y^2 + u^2\left(\frac{A(E_c)}{A(E_f)}\right)\Big/\left(\frac{A(E_c)}{A(E_f)}\right)^2 + u^2\left(\frac{I_\gamma(E_f)}{I_\gamma(E_c)}\right)\Big/\left(\frac{I_\gamma(E_f)}{I_\gamma(E_c)}\right)^2 + u^2\left(\frac{R^p(E_f)}{R^p(E_c)}\right)\Big/\left(\frac{R^p(E_f)}{R^p(E_c)}\right)^2 + u^2\left(\frac{T(E_f)}{T(E_c)}\right)\Big/\left(\frac{T(E_f)}{T(E_c)}\right)^2$$

3. EXPERIMENTAL RESULTS

3.1 Description of the experiments

To check the consistency of measurements and to reduce the final uncertainty, the capture rates are obtained from at least 2 characteristic γ-rays and the fission rates from 2 to 5 fission products with independent mass chains. Series of 5 to 12 acquisitions per sample are performed to check the reproducibility of measurements and especially the correctness of the decay and the dead time corrections. Measurement times are adapted to reduce the statistical uncertainty on countings below 0.5%. Tab. 1 resumes the main measurement information.

Table 1 : Description of the measurements

Sample	Irradiation conditions	Number of measurements	Cumulative Measurement time	Capture rate characteristic γ-rays	Fission rate characteristic γ-rays
^{232}Th	(80 W, 3 h)	12	14 h	300.1 keV (^{233}Pa) 312.0 keV (^{233}Pa)	293.3 keV (^{143}Ce) 487.0 keV (^{140}La) 954.5 keV (^{132}I) 1596.2 keV (^{140}La)
^{237}Np	(80 W, 2 h)	11	36 h	984.5 keV (^{238}Np) 1028.6 keV (^{238}Np)	293.3 keV (^{143}Ce) 487.0 keV (^{140}La) 954.5 keV (^{132}I) 1596.2 keV (^{140}La)
^{242}Pu	(80 W, 2 h)	7	14 h	84.0 keV (^{243}Pu) 381.7 keV (^{243}Pu)	293.3 keV (^{143}Ce) 1260.4 keV (^{135}I)

3.2 Saturated count rate measurements

3.2.1 Net peak area measurements

Fig. 3 presents a typical γ-ray spectrum obtained after a cooling time of 1 day. The GENIE 2000 software is used for the analysis of spectrum.

Figure 3 : γ-ray spectrum of the ^{232}Th sample, one day after the irradiation.

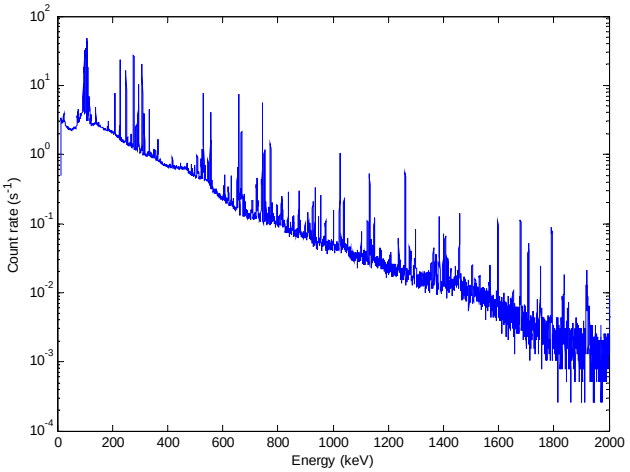

3.2.2 Decay correction

The decay correction factor C_{dec} represents the ratio between the saturated count rate (activity obtained after an infinite time of irradiation before any decay) and the measured count rate. Its expression depends on the filiation of the nuclide, and can be written as:

- $$C_{dec} = \frac{\lambda_x t_r}{\exp(-\lambda_x t_o)(1-\exp(-\lambda_x t_i))(1-\exp(-\lambda_x t_r))} \quad (3),$$
  in the case of filiations of the 1st order, i.e. for all the nuclides with a pure exponential decay (where t_i, t_o, t_r are respectively the irradiation, cooling and measurement time);
- $$C_{dec} = \frac{(\lambda_x - \lambda_w)t_r}{\frac{\lambda_x}{\lambda_w}\exp(-\lambda_w t_o)(1-\exp(-\lambda_w t_i))(1-\exp(-\lambda_w t_r)) - \frac{\lambda_w}{\lambda_x}\exp(-\lambda_x t_o)(1-\exp(-\lambda_x t_i))(1-\exp(-\lambda_x t_r))} \quad (4),$$
  in the case of filiations of the 2nd order, i.e. for all the nuclides 'X' with a competition between its decay and the one of his father 'W'.

The uncertainty on the decay correction factor is calculated with the variance propagation relation [7]. It mainly comes from nuclear data, which, for the studied nuclides, are known at better than 0.5%, leading to a similar uncertainty on the C_{dec} factor.

3.2.3 Dead time correction

In order to adapt the live time correction to the measurement of short-life nuclides, a study of the dead time as a function of time has been necessary. It has shown a good consistency with the sum of two purely exponential decays with specific decay constants b_1 and b_2 [8]. This study leads to the evaluation of a correction factor ξ to apply to the dead time θ, depending on C_{dec}, b_1 and b_2. Finally the dead time correction factor is :

$$C_\theta = \frac{1}{1-\xi\theta} \quad (5) \qquad \text{with } \xi \to 1 \text{ when } \lambda_X t_r \to 0$$

where θ is the mean dead time during measurement.

The correctness of pile-up rejection performed by the DSP2060 numerical system has been

checked using the standard "two sources" technique with a reference static ^{60}Co source and a perturbing ^{133}Ba source. A comparison between repeatability and reproducibility variances leads to a majoring of the error of about 0.2% up to 150 000 counts per second.

As the spectral indices only depend on the ratio of C_θ, the propagated uncertainty is supposed to be negligible compared to other sources of uncertainty.

3.2.4 Combination of several measurements

The final result of the saturated count rate is given by a weighted average of the *n* results :

$$\frac{\overline{A(E_c)}}{\overline{A(E_f)}} = \sum_{i=1}^{n} w_i \frac{A_i(E_c)}{A_i(E_f)} \Big/ \sum_{i=1}^{n} w_i \qquad (6)$$

The w_i weights are linked to the uncertainty on each measurement, and can be written as:

$$w_i = 1 \Big/ u^2\left(\frac{A_i^2(E_c)}{A_i^2(E_f)}\right) = 1 \Big/ \frac{A_i^2(E_c)}{A_i^2(E_f)}\left(\frac{u^2(N_i(E_c))}{N_i^2(E_c)} + \frac{u^2(N_i(E_f))}{N_i^2(E_f)} + \frac{u^2(C_{dec_{i,c}})}{C_{dec_{i,c}}^2} + \frac{u^2(C_{dec_{i,f}})}{C_{dec_{i,f}}^2}\right) \qquad (7)$$

The uncertainty on the weighted mean value is calculated from the internal variance, by taking into account the variance from each measurement :

$$u_{int}^2\left(\frac{\overline{A(E_c)}}{\overline{A(E_f)}}\right) = 1 \Big/ \sum_{i=1}^{n} w_i + \left[2 \Big/ \left(\sum_{i=1}^{n} w_i\right)^2 \times \sum_{i=1}^{n-1}\sum_{j=i+1}^{n} w_i w_j u(C_{dec_i}, C_{dec_j})\right]_{capture} + \left[2 \Big/ \left(\sum_{i=1}^{n} w_i\right)^2 \times \sum_{i=1}^{n-1}\sum_{j=i+1}^{n} w_i w_j u(C_{dec_i}, C_{dec_j})\right]_{fission} \qquad (8)$$

3.3 Point source efficiency calibration of the detector

The efficiency $R^P(E) = \frac{n^P(E)}{A I_\gamma(E)}$ of the detector is defined as the ratio of the photopeak count rate $n^P(E)$ to the total photonic emission $A I_\gamma(E)$. The calibration is performed using 10 mono-energetic point sources (^{241}Am, ^{109}Cd, ^{57}Co, ^{139}Ce, ^{51}Cr, ^{113}Sn, ^{137}Cs, ^{85}Sr, ^{65}Zn, ^{54}Mn) and 4 multi γ-rays point sources (^{60}Co, ^{88}Y, ^{133}Ba, ^{152}Eu), covering the range [14 - 1836 keV]. The series of data is fitted by a standard logarithmic model, with a least square method [9]:

$$\log\left(R^P(E)\right) = \sum_{i=0}^{n} a_i \log\left(\frac{E}{E_m}\right) \qquad (10)$$

where E_m is a constant chosen in the mid energy range.

Fig.4 shows an example of efficiency curve obtained with a logarithmic polynomial fitting. Tab. 2 gives some efficiency ratios and their corresponding uncertainties.

Figure 4 : Efficiency curve obtained for LEGe detector from 14 calibration sources

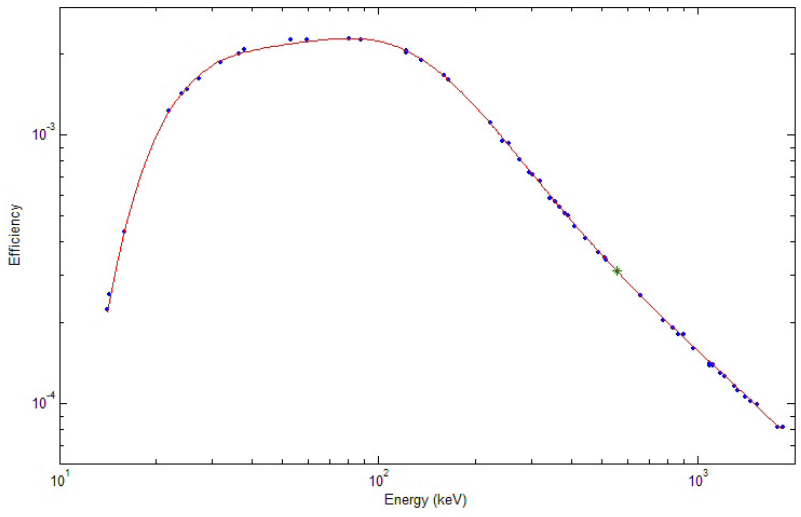

The uncertainty from each point is propagated to any interpolated value, taking into account all the variances and covariances linked to the activity of the sources, the emission probabilities of the studied γ-ray and the statistics on the counting of the peaks [7].

Table 2 : Examples of measured ratios of efficiencies

E_c	E_f	$R^P(E_c)/R^P(E_f)$	$U\left(R^P(E_c)/R^P(E_f)\right)\Big\vert_{total}$	$U\left(R^P(E_c)/R^P(E_f)\right)\Big\vert_{model}$
84.0 keV (^{243}Pu)	293.3 keV (^{143}Ce)	0.3277	0.63%	0.24%
312.0 keV (^{233}Pa)	487.0 keV (^{140}La)	0.5411	0.30%	0.23%

Thanks to a precise variance propagation with basic correlations between efficiencies from multi γ-rays and mono-energetic sources, the uncertainty on the ratio of the efficiencies was significantly reduced (< 0.7%), compared with past studies (~ 2%) [2].

3.4 Efficiency transfer calculations

Efficiency transfer corrections are used to correct the self-absorption phenomena inside the fuel samples and to take into account changes in the average incidence angle of photons due to the measurement of a volumic source, compared to the point source calibration. These factors are calculated, for all energies of emitted γ-rays and for all studied samples, with the MCNP4C2 code, using the energy deposit tally "F8" [10] [11]. The calculation scheme includes the description of the real geometry of the spectrometry device. A preliminary calculation with the APOLLO2 code (+ JEF2.2), is done to estimate the radial heterogeneity of photon sources inside the fuel pin. Fig.5 shows some calculated reaction rate distributions.

Figure 5 : Fission rate (left side) and capture rate (right side) distribution inside the irradiated ^{242}Pu fuel sample, calculated with the APOLLO2 code and the JEF2.2 library.

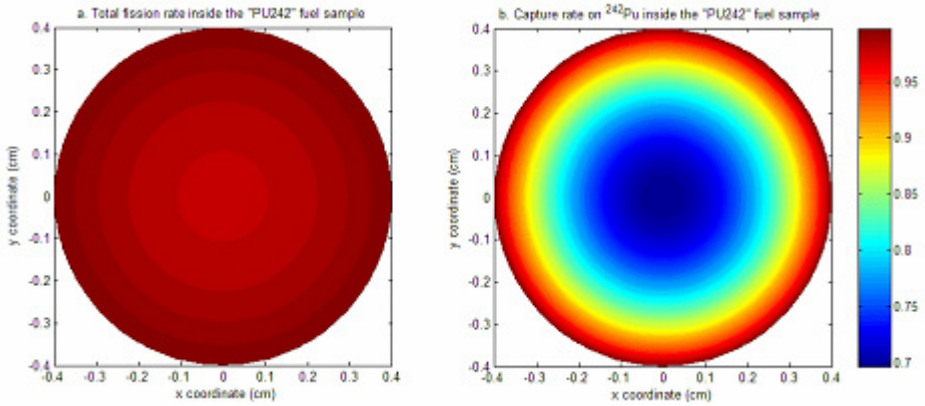

A perturbation tally is also used to study the influence of the density on self-absorption. Based on chemical analysis of each sample, it can vary from 0.1 to 0.7%. Then, the ratio of efficiency transfer corrections is obtained by :

$$T(E_c)/T(E_f) = \left(\eta_V(E_c)/\eta_o(E_c)\right)/\left(\eta_V(E_f)/\eta_o(E_f)\right) \quad (11),$$

where $\eta_V(E)$ and $\eta_o(E)$ are the results of MCNP4C2 calculations, respectively for a volumic source inside the fuel sample and for a point source, with the energy E.

Tab. 3 presents some calculated ratios for several capture and fission products. The associated uncertainties are estimated taking into account the statistical convergence u_c of Monte Carlo calculations and from the uncertainty $u(d)$ on the sample density [7].

Table 3 : Examples of calculated ratios of efficiency transfer corrections

E_c	E_f	$T(E_c)/T(E_f)$	$U(T(E_c)/T(E_f))\|_{total}$	$U(T(E_c)/T(E_f))\|_{density}$	$U(T(E_c)/T(E_f))\|_{Dopant\ Rate}$
84.0 keV (^{243}Pu)	293.3 keV (^{143}Ce)	0.1.067	0.35%	0.03%	< 0.01%
312.0 keV (^{233}Pa)	487.0 keV (^{140}La)	0.5.811	0.35%	0.07%	0.03%

3.5 Average fission yield calculations

As the total fission rate in samples is due both to the ^{235}U thermal fission and to the ^{238}U fast fission, nuclear data from different nuclides and different energy groups have to be combined to produce an average fission yield. This leads to the following equation [12] :

$$\overline{Y} = \sum_{isotope\ i} \tau_{i,th} Y_{i,th} + \sum_{isotope\ i} \tau_{i,f} Y_{i,f} + \sum_{isotope\ i} \tau_{i,h} Y_{i,h} \quad (12)$$

with : $Y_{i,x}$ = fission yield of the nuclide 'i' for the energy group 'x',

$\tau_{i,x}$ = ratio of the fission rate from the nuclide 'i' and the energy group 'x', to the total fission rate. The indices '*th*', '*f*' and '*h*' refer to thermal, fast and high energy groups.

The $\tau_{i,x}$ coefficients are obtained using the APOLLO2 + JEF2.2 calculation scheme used for the previous reaction rate distribution studies. The fission yields for each nuclide and energy group are extracted from the JEF2.2, ENDF/B-VI.8 and JEFF3.1 libraries. Tab. 4 presents examples of average fission yields in the case of the ^{232}Th sample.

The uncertainty on the average fission yield is calculated taking into account the isotopic Uranium composition and the used nuclear data [7].

Table 4 : Examples of average fission yields for the ^{232}Th sample

Fission product	*JEF2.2 library*		*ENDF/B-VI.8 library*		*JEFF3.1 library*	
	$\overline{Y}$	$u(\overline{Y})/Y$	$\overline{Y}$	$u(\overline{Y})/Y$	$\overline{Y}$	$u(\overline{Y})/Y$
^{103}Ru	3.575×10^{-2}	5.39%	3.617×10^{-2}	1.06%	3.631×10^{-2}	1.94%
^{132}I	4.399×10^{-2}	0.91%	4.449×10^{-2}	1.15%	4.367×10^{-2}	1.07%
^{135}I	6.350×10^{-2}	2.79%	6.397×10^{-2}	1.19%	6.384×10^{-2}	2.91%
^{140}La	6.170×10^{-2}	1.56%	6.135×10^{-2}	0.84%	6.244×10^{-2}	1.26%
^{143}Ce	5.736×10^{-2}	6.37%	5.709×10^{-2}	1.21%	5.715×10^{-2}	1.24%

3.6 Spectral indices results

Tab. 5 shows a typical set of spectral indices obtained for the ^{232}Th sample, from 2 capture rate characteristic γ-rays and 5 fission rate characteristic γ-rays, using the JEF2.2, ENDF/B-VI.8 and JEFF3.1 libraries for half-lives, emission probabilities and fission yields.

Some interesting trends on the used nuclear data can be identified from the discrepancies of the individual results around their weighted average.

For example, the comparison of the ^{132}I results with the ^{143}Ce and ^{140}La results shows a better consistency when using the JEFF3.1 data. This discrepancy comes from a ~ 3% lower emission probability and a ~1.5% lower average fission yield compared with the JEF2.2 and ENDF/B-VI.8 data. From these trends, JEFF3.1 data for this nuclide seem to be more reliable.

With the same approach for every studied sample, consistent results on the basis of a 2σ total uncertainty are combined altogether to reduce the final uncertainty. Average spectral indices are calculated using a weighted average of these results, assuming that (a) the efficiency ratios are fully correlated altogether as they are evaluated from the same experimental curve, (b) the γ-rays coming from the same nuclide are fully correlated in

emission probabilities, (c) the fission product yields are not correlated for nuclides with different mass numbers, (d) the efficiency transfer corrections are not correlated as most of the uncertainty comes from the statistical convergence of Monte Carlo calculations.

Table 5 : Measured spectral indices for the ^{232}Th sample

Capture rate characteristic γ-rays	Fission rate characteristic γ-rays	*JEF2.2 library*		*ENDF/B-VI.8 library*		*JEFF3.1 library*	
		$\frac{C_x}{F}$	$u(\frac{\overline{C_x}}{F})/\frac{C_x}{F}$	$\frac{C_x}{F}$	$u(\frac{\overline{C_x}}{F})/\frac{C_x}{F}$	$\frac{C_x}{F}$	$u(\frac{\overline{C_x}}{F})/\frac{C_x}{F}$
^{233}Pa (300.12 keV)	^{143}Ce (293.3 keV)	0.2255	7.86%	0.2291	2.35%	0.2300	2.33%
	^{140}La (487.0 keV)	0.2350	2.96%	0.2256	2.63%	0.2361	2.35%
	^{140}La (1596.2 keV)	0.2297	2.83%	0.2286	1.99%	0.2327	2.20%
	^{132}I (954.5 keV)	0.2419	4.41%	0.2449	4.05%	0.2356	3.64%
^{233}Pa (311.98 keV)	^{143}Ce (293.3 keV)	0.2200	7.66%	0.2230	1.97%	0.2235	1.77%
	^{140}La (487.0 keV)	0.2280	2.35%	0.2183	2.30%	0.2281	1.98%
	^{140}La (1596.2 keV)	0.2234	2.19%	0.2218	1.53%	0.2254	1.81%
	^{132}I (954.5 keV)	0.2367	4.04%	0.2391	3.85%	0.2315	3.42%

The final results are reported in Tab. 6. The last column indicates the experimental part of the total uncertainty, including the net peak area measurements and the efficiency calibration.

Table 6 : Final measured spectral indices

Sample	*JEF2.2 library*		*ENDF/B-VI.8 library*		*JEFF3.1 library*		
	$\frac{\overline{C_x}}{F}$	$u(\frac{\overline{C_x}}{F})/\frac{C_x}{F}$	$\frac{\overline{C_x}}{F}$	$u(\frac{\overline{C_x}}{F})/\frac{C_x}{F}$	$\frac{\overline{C_x}}{F}$	$u(\frac{\overline{C_x}}{F})/\frac{C_x}{F}$	$u(\frac{\overline{C_x}}{F})/\frac{C_x}{F}\Big\vert_{exp}$
^{232}Th	0.2280	2.12%	0.2246	1.35%	0.2278	1.46%	0.55%
^{237}Np	0.8902	3.71%	0.8763	3.61%	0.8912	3.58%	0.37%
^{242}Pu	0.2311	10.7%	0.2346	10.1%	0.2366	10.1%	1.7%

4. Calculation results

Calculations are performed with the APOLLO2 code with the JEF2.2 and JEFF3.1 libraries and with the MCNP4C2 code with the JEF2.2, ENDF/B-VI.8 and JEFF3.1 libraries. They are compared with experimental results obtained from the same nuclear data library (see Tab. 7).

Table 7 : Final deterministic calculation to experiment ratios

Sample	*MCNP4C2 + JEF2.2*		*MCNP4C2 + ENDF-B6.8*		*MCNP4C2 + JEFF3.1*		*APOLLO2 + JEF2.2*		*APOLLO2 + JEFF3.1*	
	C/E	$\frac{u(C/E)}{C/E}$	*C/E*	*C/E*	$\frac{u(C/E)}{C/E}$	*C/E*	C/E	$\frac{u(C/E)}{C/E}$	C/E	$\frac{u(C/E)}{C/E}$
^{232}Th	1.008	2.56%	1.031	2.59%	0.997	2.03%	0.994	2.35%	N.A. (a)	N.A. (a)
^{237}Np	1.085	3.92%	1.188	3.81%	1.011	3.80%	1.079	3.70%	1.011	3.70%
^{242}Pu	1.187	10.9%	1.178	10.3%	1.163	10.3%	1.188	10.9%	1.157	10.1%

(a) currently Not Available

The composition of samples is based on chemical analysis of the dopant mass ratio, which are known at around 1%. The reported uncertainty on the C/E ratio includes the uncertainties on the chemical analysis, the measurements, and the Monte Carlo calculations convergence (from 0.5% to 2%, depending on the cross section).

5. Discussions

First, C/E results in Tab.7 show an excellent agreement within 2σ of the Monte Carlo statistical convergence between deterministic and reference probabilistic calculations. These results tend to validate the used APOLLO2 calculation scheme.

Besides, the analysis of the trends on the C/Es is not consistent within the uncertainties for several isotopes and libraries. As the uncertainty on the experiment and the dopant mass ratio analysis are both around 1%, these trends have two possible explanations : (a) errors on the gamma emission probabilities of the capture product, (b) errors on the (n,γ) cross section.

In the case of ^{232}Th, all the libraries lead to good calculation to experiment agreements. The best consistency is obtained from the JEFF3.1 one with a very accurate experimental qualification at 2%. This result has many interests for the thorium fuel cycle concepts where a high precision in the production of ^{233}U by (n,γ) capture on ^{232}Th is necessary.

In the case of ^{237}Np, very interesting trends can be observed. In fact, the thermal capture cross section in the JEF2.2 and ENDF/B-VI.8 libraries has decreased by 12% in JEFF3.1. This new evaluation leads to a consistency better than 1σ of the reported uncertainty with the experiment. This trend is also consistent with recent activation analysis measurements [13]. However, measurements by the oscillation technique, performed in the same conditions in the MINERVE facility in the framework of the OSMOSE program [1] [5] [6], show inconsistent results with the above ones. Indeed it is shown that the calculation of the integral (in the R1-UO2 lattice) (n,γ) capture cross section of ^{237}Np underestimates the experimental results by 13% (± 2%) with JEFF3.1, and by 9% (± 2%) with JEF2.2. Considering the high level of confidence in the measurements by the oscillation technique, it could be concluded that the gamma emission probabilities on the 2 studied γ-rays of ^{238}Np (0.278 at 984.5 keV and 0.203 at 1028.6 keV) are overestimated in the JEFF3.1, JEF2.2 and ENDF-B6.8 data libraries. This trend is confirmed by very recent evaluations [14], leading to about 10% smaller gamma emission probabilities of ^{238}Np (0.2519 at 984.5 keV and 0.1829 at 1028.6 keV). Taking into account these new gamma emission probabilities values for treating the experimental results presented in this paper, leads to confirm the oscillation measurements results, i.e. to an underestimation of the integral (n,γ) capture cross section of ^{237}Np.

At last, in the case of ^{242}Pu, a systematical overestimation of 16% to 19% is observed for all libraries. As the capture cross section from oscillation measurements in the OSMOSE program at about 4% [5], the C/E ratio might be representative of an error on the gamma emission probabilities. In particular, the associated normalization factor is not known at better than 9% as only one measurement was performed in the past. This shows the need to undertake further studies on the ^{243}Pu decay data.

6. CONCLUSIONS

In this study, an new experimental γ-ray spectrometry technique has been developed for the qualification of relevant nuclear data of minor actinides. The repetition of the measurements, the use of several characteristic γ-rays per reaction rate, and a very precise calibration of the HPGe detector over the full energy range, allowed very high accuracy (< 2%) measurements.

Significant calculation to experiment ratios are obtained, both from deterministic APOLLO2 code calculations and probabilistic MCNP4C2 calculations with the JEF2.2, ENDF/B-VI.8 and JEFF3.1 libraries.

It is shown that for all data libraries, the agreement between calculations and experiments is excellent for ^{232}Th.

In the case of ^{237}Np, using the comparison with oscillation measurements also performed

during the OSMOSE program, it is concluded that the gamma emission probabilities of the 2 major γ-rays of ^{238}Np are overestimated by about 10% in the JEFF3.1, JEF2.2 and ENDF-B6.8 libraries, and that the integral (n,γ) capture cross section of ^{237}Np is underestimated by about 10%.

As for ^{242}Pu, an overestimation of the gamma emission probabilities tends to be shown. However, the current uncertainty on these data in the main libraries is so high (about 9%) that it is not possible to conclude definitely. Further studies should be undertaken to progress on these correlations.

References

1) JP. Hudelot, R. Klann, P. Fougeras, F. Jorion, N. Drin, L. Donnet, "OSMOSE : An experimental Program for the Qualification of Integral Cross Sections of Actinides", PHYSOR 2004 Conference, Chicago (US), 2004
2) JP. Hudelot, P. Fougeras, S. Cathalau, "Measurement of the modified conversion ratio of ^{238}U by gamma-ray spectrometry on an irradiated fuel pin", Proceedings of the 11th international Symposium Capture Gamma-Ray Spectroscopy and Related Topics, Pruhonice, Czech Republic, 2-6 September 2002.
3) Los Alamos Monte Carlo Group, JF. Briesmeister (Editor), "MCNP – A General Monte Carlo N-Particle Transport Code", Los Alamos National Laboratory, Manual LA-13709-M, March 2000
4) A. Santamarina, and Al., "Qualification of the APOLLO2.5/CEA93.V6 Code for UOX and MOX fuelled PWRs", PHYSOR 2002 Conference, Seoul (Korea), 7-10 October 2002
5) D. Bernard, A. Courcelle, and Al., "Validation of Actinide Neutron Induced Cross-sections: Preliminary Analysis of the OSMOSE experiment in MINERVE", PHYSOR 2006 Conference, 2006 September 10-14, Vancouver, BC, Canada
6) JP. Hudelot, R.T. Klann, D. Bernard, M. Antony, and Al., "Preliminary Experimental Results of the OSMOSE Program for the Qualification of Integral Cross Sections of Actinides", PHYSOR 2006 Conference, 2006 September 10-14, Vancouver, BC, Canada
7) P. Leconte, JP. Hudelot, M. Antony, "Integral capture rate measurements of isotopes by γ-ray spectrometry on specific fuel samples", IYNC Conference, Stockholm, Sweden, 18-23 June 2006
8) J. Adam, AG. Belov, and Al, "Precision half-life measurement of ^{140}La with Ge-detector", Nuclear Instruments and Methods in Physics Research, 2002
9) GL. Molnar, Zs Revay, T. Belgya, "Wide energy range efficiency calibration method for Ge detectors", Nuclear Instruments and Methods in Physics Research, March 2002
10) M. Jurado Vargas, and Al., "Efficiency transfer in the calibration of a coaxial p-type HPGe detector using the Monte Carlo method", Applied Radiation and Isotopes, March 2003
11) J. Saegusa, T. Oishi, and Al., "Determination of Gamma-ray Efficiency Curves for Volume Samples by the Combination of Monte Carlo Simulations and Point Source Calibration", Journal of Nuclear Science and Technology, December 2000
12) R. Mills, "Recommendation for the use of energy dependent JEF2.2 fission product yields", Nuclear Energy Agency Data Bank, JEF/DOC-629, October 1999
13) T. Katoh, S. Nakamura, K. Furutaka, H. Harada, T. Baba, T. Fuji, H. Yamana, "Measurement of Thermal Neutron Capture Cross Section and Resonance Integral of the ^{237}Np(n,γ)^{238}Np Reaction", Journal of Nuclear Science and Technology, August 2003
14) BNL Homepage, http://www.nndc.bnl.gov/nudat2/chartNuc.jsp